

# Effects of titanium (Ti) contents on the wear resistance of low-alloy steel alloys

*Nozimjon Kholmiraev*<sup>1\*</sup>, *Nodir Turakhodjaev*<sup>1</sup>, *Nosir Saidmakhamadov*<sup>1</sup>,  
*Jamshidbek Khasanov*<sup>2</sup>, *Abdujalol Bektemirov*<sup>2</sup>, and *Nargiza Sadikova*<sup>1</sup>

<sup>1</sup>Tashkent State Technical University, Foundry technologies department, Tashkent, 700057, Uzbekistan

<sup>2</sup>Andijan Machine Building Institute, Materials science and technology of new materials department, Andijan, 170100, Uzbekistan

**Abstract.** In this study, the impact of titanium (Ti) on low-alloy steel alloys is examined, focusing on the mechanical properties of the alloy with varying Ti content levels. Heat treatment was conducted to enhance the mechanical properties and performance indicators of the casting samples. The elemental volume distribution mapping and microstructure analysis of the research samples were performed using SEM - Carl Zeiss Ultra Plus Field Emission. Subsequently, the hardness and wear resistance characteristics of samples containing Ti contents of 0, 0.1, 0.3, 0.5, 0.8, and 1.1 were evaluated post heat treatment. Notably, steel samples containing 0.3% and 0.5% Ti, exhibiting structures of ferrite, martensite, and limited bainite, demonstrated superior hardness and wear resistance properties. Abrasive wear resistance tests were conducted using a specialized device with a horizontal diamond disc. The primary objective of this research is to introduce the developed technology for the rolling mill rolls at a prominent metal manufacturing enterprise in the republic, resulting in enhanced economic efficiency through increased production volume. Consequently, achieving a hardness of HB 323 and improving wear resistance by 1.2 times were notable outcomes of the study.

## 1 Introduction

Alloyed steels are divided into 3 types according to the number of alloying elements in the alloy: The content of type 1 alloying elements no more than 2.5 %. They are low – alloyed steels and belong to the class of construction steels. Alloying elements included in type 2 range from 2.5 to 10%. They are medium alloyed steels and belong to the class of construction and tool steels. Also, steels with more than 10% of alloying elements included in 3 types. They are multi – alloyed steels and belong to the classes of special properties steels.

High strength low – alloy steels. These steels are better mechanical properties and wear resistance than ordinary structural carbon steels. Because they are designed to respond not to chemical composition, but to specific mechanical properties. High-strength low – alloy steels

---

\* Corresponding author: [xolmirzayev\\_nozimjon@mail.ru](mailto:xolmirzayev_nozimjon@mail.ru)

have a low carbon content (0.05 – 0.25% C), and a manganese content of up to 2.0%. Contains small amounts of elements such as chromium, nickel, molybdenum, copper, nitrogen, vanadium, niobium, titanium and zirconium. For many low – alloy steels, the main function of alloying elements is to increase the mechanical properties of the material after heat treatment [1, 2].

Compared to high – manganese and high – alloyed steels, low – alloyed steels contain alloying elements with low cost. In addition, mechanical cutting is convenient and has the ability to re-liquefy. Furthermore, it is possible to create different types of microstructures by choosing the parameters of the heat treatment mode based on the chemical composition of the alloy.

In world practice, scientific and research studies on the effect of Ti element on impact wear resistance of high-strength low-alloy steel alloys were carried out by the world's leading scientists, including Li, Shuying, et al. considered in the studies of [3-5]. In the carried out scientific and research works, samples with 0, 0.04, 0.1 and 2.0% Ti content were analyzed for low-alloyed steel alloys. As a result, the mechanical properties of the 0.04% titanium steel alloy including the formation of martensite and lower bainite structures are improved. In addition, the alloy with 2.0% titanium showed the lowest wear resistance among all samples. As a result, the technology of improving wear resistance of the alloy based on structure formation was developed. Huang, Long, et al [6-8] Melting of TiC-strengthened low-alloy martensitic wear-resistant steel alloys, modification with TiC in both nano and micron sizes in furnace, improving wear resistance without increasing hardness through heat treatment processes in the cast alloy, in this research, the wear resistance of low-alloy steel alloy was increased by 1.35 times when it was modified only with micron-sized TiC particles. In addition, technologies have been developed that improve the wear resistance of low-alloy steel alloy was increased by 1.5 times when it was modified with micron and nano sized TiC particles. However, the effect of modification of low-alloy steel alloy with TiC on its physical, mechanical and operational parameters has not been sufficiently studied. Kostryzhev, A. G., et al. [9-10] They conducted scientific research on the effect of microalloying martensitic steels with Ti element on its wear resistance. In this work, technologies for increasing hardness and wear resistance were developed as a result of the simultaneous formation of coarse TiMoVCN, fine TiC and Fe<sub>3</sub>C particles.

## 2 Materials and methods

A new chemical composition of the alloy and liquefaction technologies were developed in the preparation of shaft details used for rolling mills made of low-alloyed steels by the casting method.

### 2.1 Liquefaction process

Low-alloyed steel alloys were liquefied in an electric arc furnace at the "Casting - Mechanics" shop of Ozmekombinat JSC, based on the new foundry technologies developed. Samples were poured for research materials. Secondary charcoal materials in low-alloy steel alloy casting, as ferroalloys from FX100A brand ferrochrome (GOST 4757-91), FMn90 brand ferromanganese (GOST 4755-91), FSi45 brand ferrosilicon (GOST 1415-93), (CaCO<sub>3</sub>) and Silicon dioxide (SiO<sub>2</sub>) were used as flux for slag production.

Secondary steel materials as charcoal materials in the casting of low-alloy steel with new chemical compositions, FeCr, FeSi, FeMn and Al were used in the specified amount based on the weight of the cast alloy [11,12].

First, a new composition was developed to change the chemical composition of low-alloy steel.

**Table 1.** Chemical composition of new low-alloy steel.

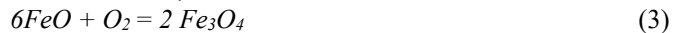
Brand	Elements, %									
	C	Si	Mn	Cr	S	P	Al	Ni	Ti	Cu
№ 1	0.35	0.7	1.2	0.8	0.04	0.04	– 0.3	–0.3	–	–0.3
№ 2	0.35	0.7	1.2	0.8	0.04	0.04	– 0.3	–0.3	0.1	–0.3
№ 3	0.35	0.7	1.2	0.8	0.04	0.04	– 0.3	–0.3	0.3	–0.3
№ 4	0.35	0.7	1.2	0.8	0.04	0.04	– 0.3	–0.3	0.5	–0.3
№ 5	0.35	0.7	1.2	0.8	0.04	0.04	– 0.3	–0.3	0.8	–0.3
№ 6	0.35	0.7	1.2	0.8	0.04	0.04	– 0.3	–0.3	1.1	–0.3

Based on the given new chemical composition, the charcoal was calculated and liquefied in an electric arc furnace.

When the metal in the furnace bath turns into a liquid state, the process of oxidation of the metal and its components and the separation of slag began. Slags are products of oxidation reactions of inclusions, non-metallic inclusions (added to the furnace as part of the charcoal), formed by the erosion of  $\text{CaCO}_3$  and refractory layer. Oxidation of additives was caused by atmospheric oxygen in the furnace.

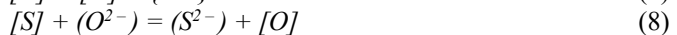
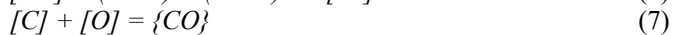
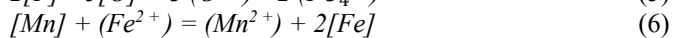
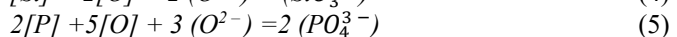
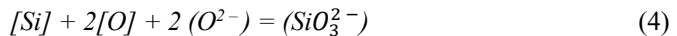


At the process temperature of this reaction, iron oxide is often further oxidized:

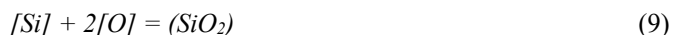


These reactions are exothermic processes, in which a significant amount of heat energy is released. The formed oxides have a high vapor pressure at the temperature inside the furnace. Some of them underwent a sublimation process or went out in the form of smoke along with exhaust gases. As a result, iron losses did not exceed 0.5% - 1.5% of the weight of the charcoal.

These reaction processes took place between the liquid metal and the arc. Firstly, silicon, phosphorus, manganese and a small amount of carbon were oxidized, and the process of desulfurization in liquid metal took place. These processes occurred as a result of the following reactions:



Due to its high affinity for oxygen, silicon was rapidly oxidized during the liquefaction of the charcoal. The oxidation reaction of silicon is usually written in a simplified form as follows:

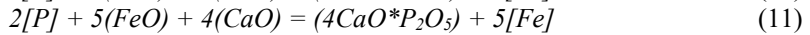
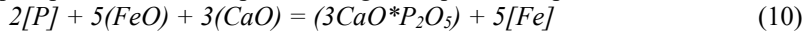


The oxidation reaction of silicon was considered exothermic. The resulting silicon oxide easily dissolves in the previous iron oxide, and as a result, the compound  $2\text{FeO} \cdot \text{SiO}_2$  is formed.

Since the content of Mn in the slag did not exceed 1%, during the liquefaction period of the charcoal, 40-80% of this element was initially oxidized. The oxidation reaction of

manganese is also exothermic, but the release of the amount of heat in it was less compared to iron.

Oxidation of phosphorus also takes place during the liquefaction period.



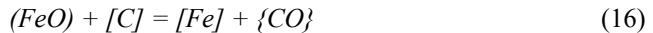
At this time, dephosphorization of liquid metal is characterized by the partition coefficient of phosphorus between metal and slag. The simplified reaction equation for phosphorus oxidation is as follows:



Oxidation of iron and other components by oxygen gas:



The reduction process of iron oxide with carbon was carried out according to the following reaction:



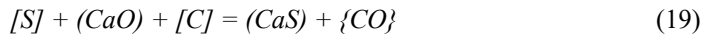
Desulfurization reaction (desulfurization) during steel liquefaction:



Sulfur does not form an oxide or complex anion in slag. "Free cations" of the elements in the slag are required for chemical bonding of the dissociated sulfur anions. The most useful is the calcium cation  $Ca^{2+}$ . Therefore, it is necessary to add sufficient amount of  $CaCO_3$  for the separation of slag during steel liquefaction [13-15].



Desulfurization of liquid metal with calcium oxide using carbon was carried out based on the following reaction equation:



Reduction reaction of oxides in slag by carbon:



As a result of the reduction reaction, iron oxide in slag was reduced by 1%, manganese and chromium oxide by 0.5%, and phosphorus by 0.01%. The chemical composition of the recycled slag consists of: CaO 50-60%,  $SiO_2$  15-20%, MgO 5-10% and  $Al_2O_3$  3-6%. At the same time, this slag has good sulfur removal properties. The desulfurization process continued as follows:



The above reduction process steps, addition of silicon and manganese content and slag reduction took a total of 15-20 minutes.

After that, samples were taken from three places by stirring the liquid metal in the furnace. Its chemical composition was sent to the central laboratory for analysis. Based on the obtained results, the differences between the composition of each element in the furnace and the composition developed for the liquidized steel grade were calculated. It was observed that it was compatible with the specified chemical composition. After that, the temperature of the liquid metal in the furnace was measured using a Heraeus digitemp-e thermocouple and it was determined to be 1640 °C, taking into account that it is enough to poured to the ladle, liquid metal was poured into a ladle heated to a temperature of 700-800 °C.

## 2.2 Microstructure, mapping and mechanical properties

After cleaning the cast samples from sand-clay molds for the purpose of research, they were first processed on a lathe in order to bring them to the specified dimensions and ensure surface cleanliness. The as-cast and heat-treated samples were sized to 15 mm × 15 mm × 60 mm for mechanical properties and structural analysis. Based on the chemical composition in Table 1, 12 samples were prepared from each of six types of steel, cast and heat-treated samples. After that, in order to smooth the surface and ensure the ease of installation on the equipment for further research, in order to use them effectively, the research samples were poured into a cylinder with a diameter of 300 mm by liquefying special granules at a specified temperature of 140 °C using the Struers CitoPress-10 device. In the optical microscopic analysis of research samples and taking microstructure images, a Struers Tegramin-30 polishing device was used for surface polishing. With the help of the device, it was processed with abrasive silicon carbide (SiC) with sizes of 200, 400, 600, 800, 1000, 1200 and 2000 μm. After that, they were cleaned with distilled water and polished with 0.3 μm nitric acid. After polishing, the samples were cleaned with alcohol. Cast samples were processed using 1% nital solution (alcohol 99%, nitric acid 1%). Duration of processing time was 24 minutes. Their surfaces, volume distribution of elements, and microstructure analyzes were analyzed using a scanning electron microscope (SEM).

Analysis of the optical microscope image of the samples during the processing of the samples on a Struers Tegramin-30 surface grinding device was carried out using the Clemex Vision Lite image analysis program on a Nikon Eclipse MA200 fast metallurgical microscope.

The process of obtaining microstructure images of research samples. A scanning electron microscope (SEM – Carl Zeiss Ultra Plus Field Emission) uses a focused beam of high-energy electrons to create various signals on the surface of samples. Electron-sample interaction signals reveal information about the sample, including external morphology, chemical composition, crystal structure, and orientation of the materials that make up the sample. Data were collected on a selected area of the sample surface and a 2D image was created showing the spatial variation in these properties. Areas 20 μm wide can be imaged using SEM techniques in scanning mode (magnification from 20X to approximately 30000X, spatial resolution from 50 to 100 nm). SEM is also capable of analyzing selected point locations in a sample; it was particularly useful in qualitative or semi-quantitative determination of chemical compositions (using EDS), crystal structure and crystal orientations (using EBSD).

In the form of SEM observation, it is possible to obtain an elemental map (liquation) of the distribution of chemical elements throughout the volume or in a defined area. The element map separates the spectral peaks at each pixel, and the elements are distributed throughout the volume with a reduced effect of overlapping peaks. There is also a quantitative element map that compensates the element map and displays the analysis results with quantitative values.

Optical emission spectroscopy or Spectrolab is considered a reliable and widely used analytical method for determining the amount of elements in all types of metal alloys. The analysis of the amount of chemical elements in the alloys obtained for the research samples was carried out on the GNR S9 Atlantis Optical Emission Spectroscopy device (Spektrolab).

Hardness test was conducted by Brinell method. Hardness determined by the Brinell method is designated as HBW.

$$HB = F/S = 2P/\pi D(D - \sqrt{D^2 - d^2}), \text{ kg/mm}^2 \quad (25)$$

D – sphere diameter, mm; F – strength, kg; S va d – trace surface left on the sample surface, mm<sup>2</sup> va diameter, mm.

The hardness of steel samples taken for research was determined. Initially, the steel sample under investigation was placed on the base, and a special ball was pressed against the steel sample using a flywheel. The spring force holding the special ball was then compressed, and the special ball compressed the sample all the way. After that, the electric motor was started and the force acting on the ball with the help of levers began to sink the ball into the sample. The steel sample was held under the force for a specified time, after which the electric motor was automatically turned off. The flywheel was twisted, a steel sample was taken, and with the help of a magnifying glass, it was measured on the perpendicular diameter based on the trace left by a special ball, and the hardness of the sample was calculated based on the formula.

### 2.3 Heat treatment process

For the experiment with the chemical composition shown in Table 1, cast shafts from low-alloy steel alloy were obtained by liquefaction in an electric arc furnace. Cast shaft details were cleaned from sand-clay moulds, surface cleanliness was ensured by mechanical processing, and they were put into a heat treatment furnace.

**Table 2.** Heat treatment.

Heating process					Quenching		Tempering		Normalization
Temperature of heat treatment furnace, °C	Temperature of heat, °C	Time, s			Quenching environment	Time, minute	Temperature of heat treatment furnace, °C	Hold on, h	
		Heating	Hold on	Total					
100–200	860–880	5 h±10 min	1 h±10 minute	6 h±10 minute	Oil	30–35	250–300	2.5	Let cool completely in the air.

Table 2 demonstrates that for the experiment, the shaft detail made of low-alloy steel was heated to a temperature of 860–880 °C for 5 hours, then it was kept at this temperature for 1 hour, and it was quenching in an oily environment for 30–35 minutes, and after being kept in the oven at a temperature below 250–300 °C for 2.5 hours, it was cooled in the open air.

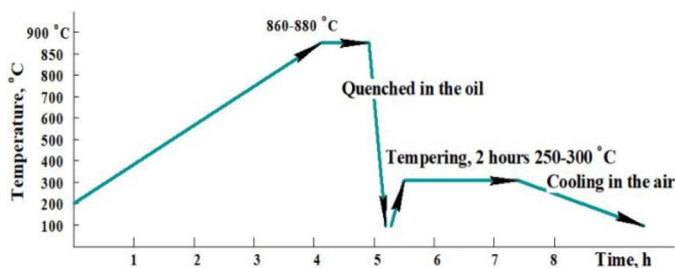


**Fig. 1.** Mode of heat treatment of research samples.

## 2.4 Abrasive wear tests

Wear resistance means the ability of a material to resist material loss as a result of some mechanical external influences.

This device can be used to determine the wear resistance of all types of metals. It's easy to use, with diamond blade speed control with automatic shut-off at a selected number of revolutions. It is designed to carry out studies of special grinding disk speeds of 400, 525, 650, 775 and 900 revolutions per minute.

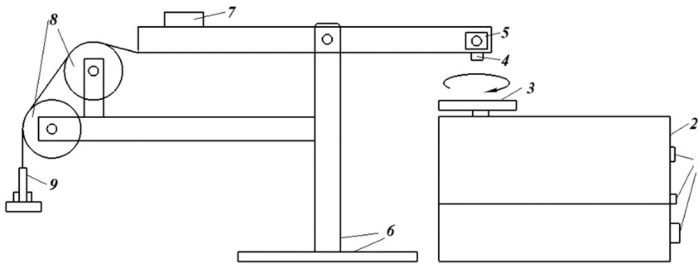


**Fig. 2.** A special device that determines the wear resistance of samples construction drawing. Structure of special equipment. 1 – control buttons; 2 – electromotive; 3 – special disk; 4 – sample under study; 5 – sample locking mechanism; 6 – supports; 7 – balancing load; 8 – rollers; 9 – loads.

Cast research samples were first prepared on a milling machine in the form of right-angled parallelepipeds, samples of uniform weight. The weight of the samples was measured using a scale before the wear resistance test, after that, samples were installed in the clamping mechanism 5. After that, under load, the diamond disc was set in motion at a specified revolution/minute speed. The samples were tested for the specified times. The wear resistance of the samples was calculated based on their weight loss per unit of time.

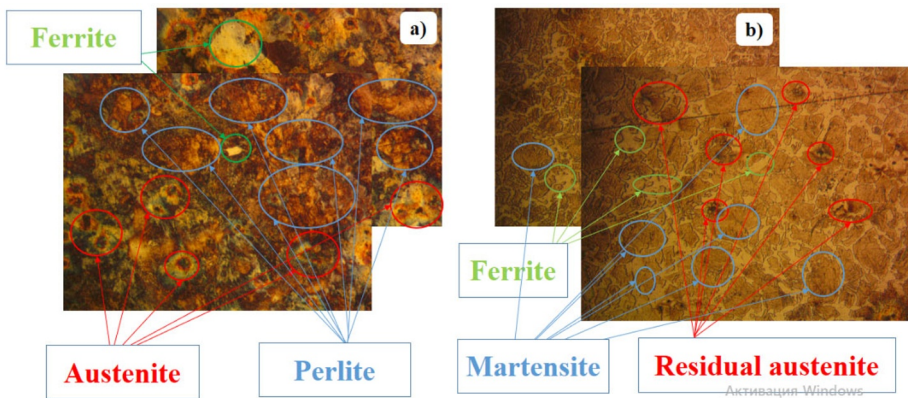
## 3 Results and discussion

### 3.1 Microstructure

FeTi was included as an alloying element in the composition of the alloy, and phases formed during the crystallization process can be seen as a eutectic. The obtained research samples were examined by SEM and the carbides present in the alloy were investigated. As a result of the observation, it was observed that TiC carbides, which were mainly distributed uniformly, were dispersed. The average diameter of the morphology of carbides in the form of TiC particles is 3 - 5  $\mu\text{m}$ , It was observed that TiC particles were evenly distributed per volume unit of the alloy as the TiC content increased.

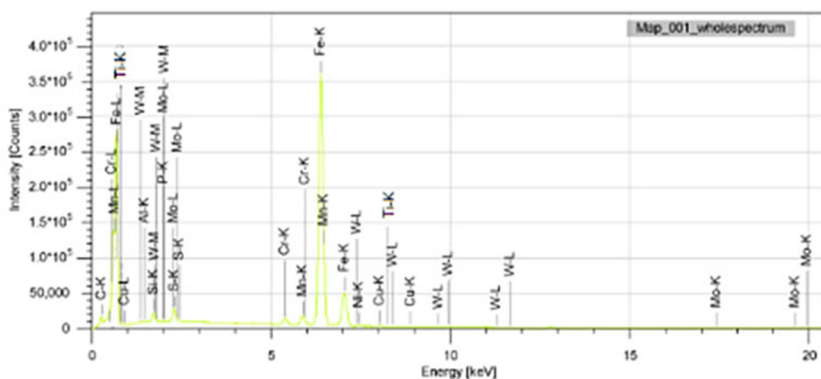
Large precipitates scattered in the alloy structure of Pic. 4 were observed. They were examined by energy dispersive X-ray spectroscopy (EDS) and found to be TiC particles. Some of the carbon atoms in the alloy matrix have reacted with titanium atoms to form TiC particles that have reduced the carbon content of the matrix. At the same time, Ti atoms also reduced the amount of C in the alloy. After heat treatment of the research samples, its microstructure mainly consisted of ferrite, lower bainite and a small amount of pearlite structures. Eutectic TiC has low density and high hardness properties, so it serves to significantly increase the wear resistance of the alloy. The effect of FeTi as an alloying element on the cast alloy based on the given suggestions is as follows, an increase in impact viscosity and dispersion of TiC carbide were observed [16-18].

On the other hand, increasing the amount of Ti in the alloy reduces its wear resistance, strength, and plasticity. The main reason for this is that during the crystallization period TiN precipitate is formed and its volume increases. Therefore, when casting steel alloys with a high content of Ti, it is recommended to keep the amount of nitrogen (N) in the liquid metal under constant control. During this period, TiN begins to precipitate in the liquid phase, but with increasing cooling rate, the maximum volume of TiN decreases gradually at the end of the solidification period. To control the size of TiN, the factor affecting the maximum size of TiN is changed to the cooling rate of the alloy in the mold, while the initial Ti and N content in the liquid steel is constant. Increasing the cooling rate of the alloy in the non-equilibrium mold reduces the temperature at the time when liquid phase TiN starts to precipitate, and the rate of TiN volume growth corresponding to lower temperatures decreases. Therefore, in addition to effectively controlling the N content during the fluidization of steel alloys, it is necessary to increase the cooling rate accordingly to reduce the amount of TiN in high-titanium steel alloys, i.e., its damage.



**Fig. 3.** Microstructure images of low alloy steel samples. a) before heat treatment, b) after heat treatment.

The images in Figure 4 show that the 0.3% titanium alloy steel alloy had a more uniform distribution of elements and less carbide formation in the research samples.



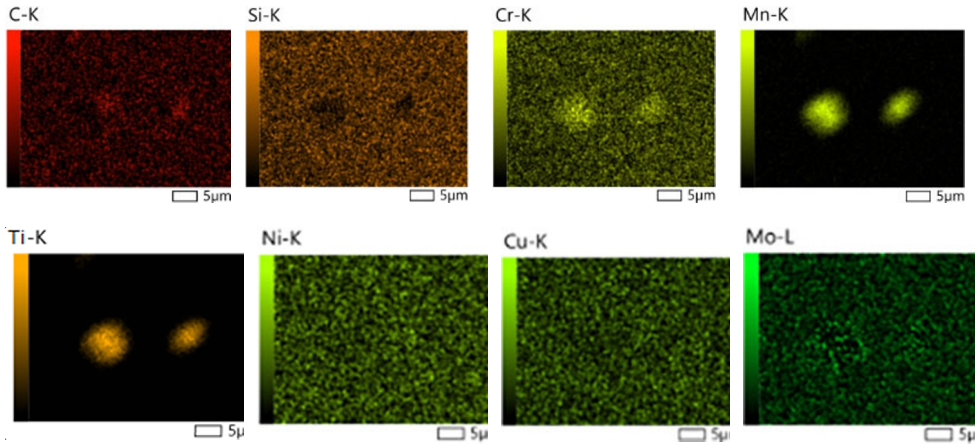


**Fig. 4.** SEM-EDS image of distribution of elements in low alloyed steel with 0.3 % Ti content before heat treatment.

### 3.2 Mechanical properties

Impact–abrasive wear performance. The cast samples were first made into uniform weighted rectangular parallelepiped samples on a milling machine. Before the wear test, the samples were weighed using a weighing scale, after which the samples were mounted on a special device with a diamond disk for determining the wear resistance. After that, the diamond disc was moved at a speed of 525 revolutions/minute under the influence of a load of 2 kg.

**Table 3.** Weight loss over time.

Time, minutes		15	20	25	30	35
Lost weight, grams	1.	0.16	0.22	0.27	0.32	0.38
	2.	0.14	0.17	0.20	0.25	0.29
	3.	0.07	0.07	0.10	0.15	0.19
	4.	0.07	0.07	0.09	0.13	0.18
	5.	0.05	0.11	0.13	0.20	0.22
	6.	0.04	0.12	0.14	0.19	0.23

Samples were tested for 15, 20, 25, 30 and 35 minutes. The weights of the samples were measured after the study for each time period.

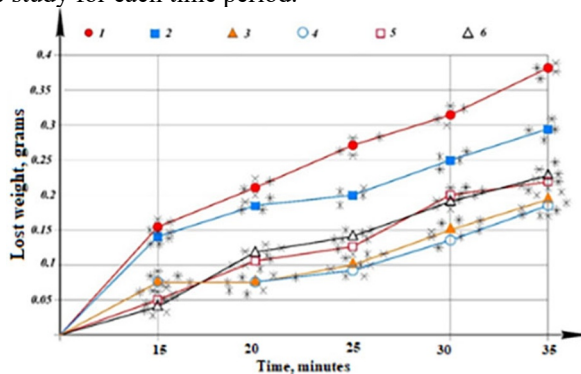


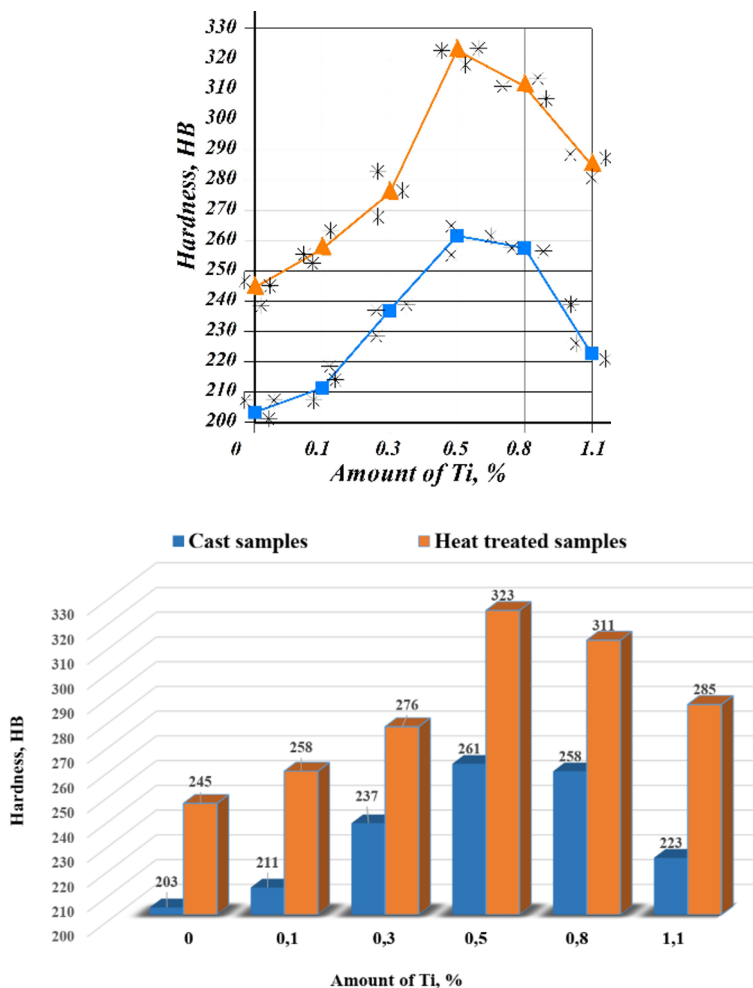
**Fig. 5.** Effect of research samples made of low-alloy steel alloys on wear resistance.

The wear resistance of the samples was calculated based on the decrease in their weight per unit of time.

Hardness. Figure 6 shows the effect of the amount of titanium on the Brinell hardness of the samples before and after heat treatment. Adding up to 0.5% of titanium in the samples increased the hardness. The maximum hardness was achieved as a result of heat treatment in samples containing 0.5% titanium. The titanium content prevents segregation of carbides along grain boundaries, and the heat treatment improved alloy hardness by redistributing carbides throughout the matrix.

**Table 4.** Hardness.

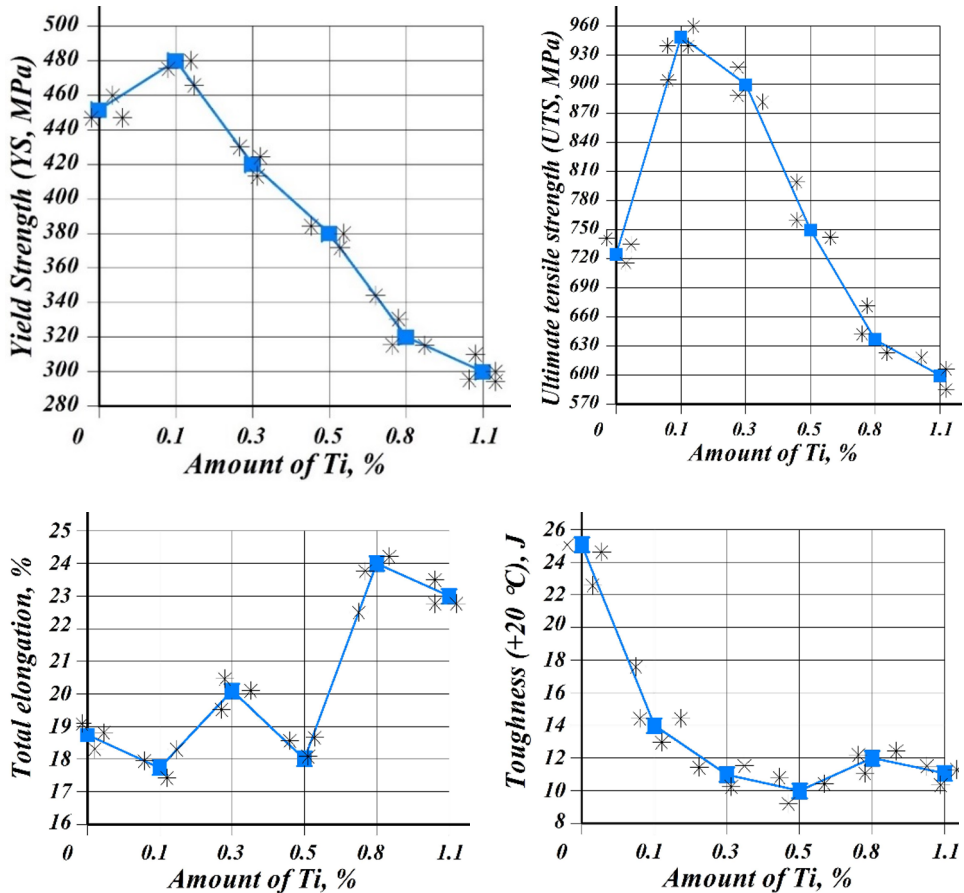
Amount of Ti		0	0.1	0.3	0.5	0.8	1.1
Hardness HB	1.	203	211	237	261	258	223
	2.	245	258	276	323	311	285



**Fig. 6.** Research analyzes before and after heat treatment according to Ti content.

**Table 5.** Table of values mechanical properties of alloy with different amounts of Ti in the composition (Yield Strength, Ultimate Tensile Strength, Total elongation, Toughness).

Parameters	Steel alloy					
	1	2	3	4	5	6
YS, MPa	450±25	480±10	420±10	380±10	320±10	300±10
UTS, MPa	725±30	950±20	900±20	750±30	640±20	600±20
Total elongation, %	18.8±0.4	17.8±0.4	20.3±0.5	18.1±0.6	24.0±0.3	23.0±0.5
Toughness (+20 °C), J	25±4	14±2	11±2	10±2	12±1	11±1

**Fig. 7.** Graphic representation of the mechanical properties of the studied samples.

## 4 Conclusion

In this research study, an analysis of the heat treatment of low-alloy steel alloys with varying titanium (Ti) concentrations is presented. The investigation delved into the microstructures, elemental mappings, mechanical properties, and primary wear resistance characteristics of the samples. The key conclusions drawn from the research findings are as follows.

Steel 1 and Steel 2, with Ti contents of 0% and 0.1%, exhibited martensite grain microstructures, while Steel 3 and Steel 4, containing 0.3% and 0.5% Ti, displayed eutectoid ferrite, martensite, and some bainite structures. Steel 5 and Steel 6, with Ti contents of 0.8%

and 1.1%, revealed the presence of small TiC and TiN precipitates. Notably, TiC particles sized 3-5  $\mu\text{m}$  were identified in Steel 3 and Steel 4.

Among the six types of low-alloyed steel alloys subjected to heat treatment, an increase in Ti content to 0.5% corresponded to proportional enhancements in hardness and wear resistance properties, achieving a maximum hardness of 323 HB.

The study observed a decrease in hardness and wear resistance properties beyond 0.5% Ti content due to Ti combining with nitrogen (N) during crystallization, forming TiN precipitates that increase in volume. To mitigate this, controlling N content during steel alloy melting and enhancing the cooling rate of the cast alloy are recommended to reduce TiN formation and associated degradation.

The research identified the optimal Ti content level for enhancing the wear resistance of low-alloy steel alloys. Abrasive wear tests on the T35SiCrMn11 steel alloy revealed that Ti concentrations of 0.3-0.5% improved wear resistance properties by 1.2-1.3 times compared to standard samples.

## References

1. W. D. Callister, D. G. Rethwisch, *Fundamentals of materials science and engineering: an integrated approach* (United States, 2007)
2. M. Kutz, *Mechanical engineers handbook* (United States, 2015)
3. S. Li, H. Yu, Y. Lu, J. Lu, W. Wang, S. Yang, *Wear* **474** 203647 (2021)
4. J. Zhao, X. Zhao, X. Zhao, C. Dong, S. Kang, *Materials Science and Engineering: A* **744**, 86-93 (2019)
5. S. Li, H. Yu, Y. Lu, J. Lu, W. Wang, S. Yang, *Wear* **474** 203647 (2021)
6. L. Huang, X. Deng, Q. Wang, Z. Wang, *ISIJ International* **60(11)**, 2586-2595 (2020)
7. S.M. Hong, E.K. Park, J.J. Park, M.K. Lee, J.G. Lee, *Mater. Sci. Eng. A* **643**, 37 (2015). <https://doi.org/10.1016/j.msea.2015.07.026>
8. L. Huang, X. Deng, Q. Wang, Z. Wang, *ISIJ International* **60(11)**, 2586-2595 (2020)
9. A.G. Kostryzhev, C.R. Killmore, D. Yu, E.V. Pereloma, *Wear* **446** 203203 (2020)
10. R. Soto, W. Saikaly, X. Bano, C. Issartel, G. Rigaut, A. Charai, *Acta Materialia* **47(12)**, 3475-3481 (1999)
11. N. Kholmiraev, N. Turakhodjaev, N. Saidmakhamadov, J. Khasanov, S. Saidkhodjaeva, N. Sadikova, *Lecture Notes in Networks and Systems* **762** LNNS (2023). [https://doi.org/10.1007/978-3-031-40628-7\\_18](https://doi.org/10.1007/978-3-031-40628-7_18)
12. S. Tursunbaev, D. Umarova, M. Kuchkorova, A. Baydullaev, *Journal of Physics: Conference Series* 2176(1) (2022). <https://doi.org/10.1088/1742-6596/2176/1/012053>
13. *Electric Arc Furnace Steelmaking*. Mirosław Karbowniczek. First edition published 2022 by CRC Press 6000 Broken Sound Parkway NW, Suite 300, Boca Raton, FL 33487-2742
14. U. Mardonov, S. Khasanov, A. Jeltukhin, S. Ozodova, *Manufacturing Technology*, **23(1)**, 73-80 (2023). <https://www.doi.org/10.21062/mft.2023.006>
15. N. Turakhodjaev, M. Akramov, S. Turakhujaeva, S. Tursunbaev, A. Turakhujaeva, J. Kamalov, *International Journal of Mechatronics and Applied Mechanics* **1(9)**, 90-95 (2021). <https://doi.org/10.17683/IJOMAM/ISSUE9.13>
16. T. Nodir, S. Nosir, S. Shokhista, O. Furkat, K. Nozimjon, B. Valida, *International Journal of Mechatronics and Applied Mechanics* **1(10)** (2021). <https://doi.org/10.17683/IJOMAM/ISSUE10/V1.19>

17. S. Nosir, K. Bokhodir, *Development of liquefaction technology 280X29NL to increase the strength and brittleness of castings*, International Conference on Reliable Systems Engineering (ICoRSE)-2022, pp. 105–115. Springer International Publishing, Cham (2022). [https://doi.org/10.1007/978-3-031-15944-2\\_10](https://doi.org/10.1007/978-3-031-15944-2_10)
18. B. Kholmurodov, M. Dzhuraeva, U. Sharafutdinov, E. Kuznecov, E3S Web of Conferences, **278**, 01025 (2021)